SUPPLEMENTARY METHODS

Immunofluorescence analysis of CHO cells

For immunofluorescence analysis, CHO cell clones were grown on glass coverslips coated with 0.1 % gelatine in phosphate-buffered saline with or without 1 ng/ml doxycycline for 24 hours and then fixed with 4% formaldehyd (10 min at room temperature). After washing, cells were subjected to standard confocal immunofluorescence microscopy using primary anti-SORLA and anti-APP 6E10 IgG and Alexa 488- and Alexa 555-conjugated secondary antibodies.

Knockdown of SORLA in SH-SY5Y cells

The neuronalblastoma cell line SH-SY5Y was grown in 6-wells in DMEM/HAM´s F12 (Gibco) supplemented with 10% fetal calf serum (FCS), non-essential amino acids, and L-glutamine. At 80% confluency, the cells were washed in phosphate buffered saline (PBS) and incubated for 24 h in 500 µl Accell delivery medium (Dharmacon Cat.# B-005000) with 1 µM of Accell siRNA directed against *SORLA* (Dharmacon Cat.# A-004722-14) . Thereafter, fresh medium was added to the cells to a final 3% FCS concentration for further 72 h, followed by complete culture medium that was conditioned for 24 h. Cells were lysed in lysis buffer (20 mM Tris-HCl, pH 8,0, 150 mM NaCl, 1% NP40, 1% Triton-X100) supplemented with protease inhibitor cocktail (cOmplete Plus, Roche, Cat.#11836170001) for 1 h on ice. Following centrifugation (15 min, 13,000 rpm, 4°C) equal volumes of protein solution were added to ELISA plates to quantify SORLA protein levels by custom-made ELISA as described below. For determination of sAPPα, sAPPβ, and Aβ, media were loaded onto ELISA plates (Meso Scale Discovery; sAPPα/sAPPβ Duplex ELISA

Cat.# K15120E; Aβ Single Plex ELISA Cat.#K150FTE) and quantified according to manufacturer's protocols.

Fluorescence correlation spectroscopy (FCS)

SH-SY5Y cells were co-transfected with expression constructs for APP-GFP and APP-RFP. Two days later, FCS measurements were performed at room temperatur on a LSM710-ConfoCor3 system (Zeiss MicroImaging, Germany) using a C-Apochromat infinity-corrected x40/1.2 water objective. Excitation of the fusion proteins was achieved by both an argon laser at 488nm (APP-GFP) and a DPSS laser at 561nm (APP-RFP), respectively. Duration of one measurement was set to 100s. Autocorrelation and cross-correlation curves were derived from the molecular dynamics using the ZEN2010 software (Zeiss MicroImaging, Germany). The curves were fitted by a two dimensional fit with two components. Only convergent curves were used for normalization to the correlation amplitude by applying the equation $G(\tau) = \langle \delta F(t) \delta F(t+\tau) \rangle / \langle F(t) \rangle^2$ where $\langle\rangle$ indicates the time avarage and $\delta F(t) = F(t) - \langle F(t) \rangle$ the dynamics around the mean intensity. Principles of FCS in conjunction with confocal laser scanning have been previously decribed in Elson EL, 2001 (Fluorescence correlation spectroscopy measures molecular transport in cells. *Traffic* **2:** 789-796).

Quantification of proteins in CHO cells

Concentrations of APP and SORLA in CHO cell lysates were determined by standard SDS-PAGE and densitometric scanning of replicate Western blots. Alternatively,

APP in cell lysates as well as APP processing products in the media were quantified using commercially available ELISA assays from Invitrogen (anti-APP #KHB0051; anti-Aβ #KHB3482) and IBL (anti-sAPPα #27734; anti-sAPPβ #27732). ELISA for sAPPβ and Aβ are specific for the respective processing products. ELISA used for detection of APP in cell lysates and of sAPPα in media potentially cross-react. However, as shown in supplementary figure 3, no soluble APP products were detected by Western blot analysis in CHO cell extracts using specific antiserum IgG 2B3 (IBL International). Also, no signal corresponding to full-length APP in the cell supernatant was seen using specific antiserum 1227. This control experiment confirmed that the immunoreactivity measured by anti-APP and sAPPα ELISA in cell extracts exclusively represented the anticipated peptides.

For quantification of SORLA, we developed a custom-made ELISA in 96-well plates (Nunc Maxisorb F96, Thermo Fisher Scientific) coated with 1 µg/ml of rabbit anti-SORLA IgG (IgG 5387) in coating buffer (100 mM sodiumbicarbonate, pH 9,8) at 4°C over night. After rinsing in wash buffer (150 mM NaCl, 7.5 mM dinatriumhydrogenphosphat, 2.8 mM natriumdihydrogenphosphat, 0.05% Tween, pH 7,4), coated wells were blocked with wash buffer supplemented with 2.5% casein (Sigma-Aldrich) at 4°C over night. Protein lysates and recombinant SORLA protein standards (purified from stably transfected CHO cells) were loaded on the wells and incubated over night at 4°C. The next day, the plates were washed and incubated with mouse monoclonal anti-SORLA antibody (IgG 20c11) at a final concentration of 1 µg/ml in wash buffer over night, and followed by rabbit anti-mouse poly-horseradish peroxidase IgG for 2 hours at room temperature (1:2500 in wash buffer; Dako). Colorimetric staining was performed by adding 100 µl peroxide buffer (Thermo

Fisher Scientific) with o-phenylenediamine (Pierce) for 30 min at room temperature and measured on an ELISA Reader at 450 nm.

Secretase assays

The SensoLyte 520 TACE Activity Assay Kit (AnaSpec) applies a QXL 520/5-FAM FRET APP substrate to measure α-secretase activity. Quenching of the fluorescence group 5-FAM by QXL 520 is released upon substrate cleavage by TACE as monitored by an increase in 5-FAM fluorescence at excitation/emission 490nm/520nm. The β-secretase activity assay kit (BioVision) utilizes a secretase-specific peptide conjugated to two reporter molecules. In the uncleaved form the fluorescent emission is quenched. After cleavage of the peptide by β-secretase the two reporter molecules physically separate allowing the release of a fluorescent signal.

To quantify γ-secretase activity, we used a PCR-based cloning approach to generate constructs encoding the signal peptide of human APP fused with sequences encoding C99 and C83. The respective fused cDNAs were inserted into pcDNA3.1hyg to derive vectors pcDNA3.1hyg SP-C83 and pcDNA3.1hyg SP-C99. Both plasmids were transiently introduced into CHO and CHO-S cells for 48 hours. Thereafter, cells were lysed in buffer A (50 mM Hepes, 150 mM NaCl, 5 mM EDTA, pH 7.4) and centrifuged for 15 min at 10,000 x g at 4°C. Pellets were resuspended in buffer B (50 mM Hepes, 150 mM NaCl, pH 7.0) supplemented with 5 mM of metalloprotease inhibitor 1-10-phenanthroline monohydrate (Sigma-Aldrich). Protein lysates were divided into two equal parts. Whereas one aliquot was kept on ice (0 time point), the second aliquot was incubated at 37°C for 2 hours. Then, lysates were centrifuged 15 min at 10,000 x g at 4°C and supernatants loaded on 15 % SDS-Tris-

Glycine polyacrylamide gels for immunodetection of C99, C83, and AICD using anti-APP IgG 1227.

***Mathematical modeling of APP processing**:*

The biochemical network consists of monomer processing (upper panel of Fig. 11A) and dimer processing (lower panel of Fig. 11A). The two modules are connected by the reversible dimerization-dissociation of APP and secretases. Two identical monomeric forms of APP and secretases dimerize to give the corresponding dimeric forms of APP and secretases. In the reverse direction, the dimeric forms of APP and secretases give the respective identical monomeric forms of APP and secretases. In both modules, the interaction of APP with α- and β-secretases leads to the formation of non-amyloidogenic (sAPPα and C83) and amyloidogenic (sAPPβ and C99) products. However, the reactants APP and secretases are in monomeric form within the monomer processing and in dimeric form within the dimer processing. The interaction between SORLA and monomeric APP lessens the amount of APP monomers available for processing and prevents the formation of APP dimers. We focused our model in such a way that the dimeric forms of the secretases only act on the dimeric form of APP and the monomeric forms of the secretases only act on the monomeric form of APP. Descriptions of the variables used in the biochemical network are provided in Table A.1. All the parameter values of the model are estimated by optimization from dose-response series for sAPPα and sAPPβ as a function of APP_{Tot} for cells with or without SORLA.

A.1. Parameter and variable descriptions

Description of the variables used in the biochemical network.

Notation	Description
APP	monomeric form of APP
α	monomeric form of α-secretase
sAPPα	soluble APPα, resulting from APP-monomer processing
C83	fragment C83, resulting from APP-monomer processing
$C_{APP\alpha}$	complex of *APP* and *α*-secretase, formed during APP-monomer processing
β	monomeric form of β-secretase
sAPPβ	soluble APPβ, resulting from APP-monomer processing
C99	fragment C99, resulting from APP-monomer processing
$C_{APP\beta}$	complex of *APP* and *β*-secretase, formed during APP-monomer processing
APP_d	dimeric form of APP
α_d	dimeric form of α-secretase
*sAPPα**	soluble APPα, resulting from APP-dimer processing
$C83_d$	fragment C83-dimer in APP-dimer processing
$C_{APP\alpha\alpha d}$	complex of *APP* and *α*-secretase in APP-dimer processing
β_d	dimeric form of β-secretase
*sAPPβ**	soluble APPβ in APP-dimer processing
$C99_d$	fragment C99-dimer in APP-dimer processing
$C_{APP\alpha\beta d}$	complex of *APP* and *β*-secretase in APP-dimer processing
SORLA	sorting protein-related receptor with A-type repeats
$C_{APPSORLA}$	complex of *APP* and *SORLA*

Description of the variables and parameters used in the mathematical model.

Notation	Unit	Description
APP	fmol	free APP-monomer
α	fmol	free α-secretase-monomer
β	fmol	free β-secretase-monomer
$C_{APP\alpha}$	fmol	complex of APP and α-secretase, formed during APP-monomer processing
$C_{APP\beta}$	fmol	complex of APP and β-secretase, formed during APP-monomer processing
$sAPP\alpha$	fmol	soluble APPα resulting from APP-monomer processing
$sAPP\beta$	fmol	soluble APPβ resulting from APP-monomer processing
APP_d	fmol	free APP-dimer
α_d	fmol	free α-secretase-dimer
β_d	fmol	free β-secretase-dimer
$C_{APP_d\alpha_d}$	fmol	complex of APP_d and α_d, formed during APP-dimer processing
$C_{APP_d\beta_d}$	fmol	complex of APP_d and β_d, formed during APP-dimer processing
$sAPP\alpha^*$	fmol	soluble APPα resulting from APP-dimer processing
$sAPP\beta^*$	fmol	soluble APPβ resulting from APP-dimer processing
$SORLA$	fmol	free sorting protein-related receptor SORLA
$C_{APPSORLA}$	fmol	complex of APP and $SORLA$
APP_{Tot}	fmol	total APP
$SORLA_{Tot}$	fmol	total SORLA conserved in the whole system
α_{Tot}	fmol	total α-secretase conserved in the whole system
β_{Tot}	fmol	total β-secretase conserved in the whole system
$sAPP\alpha_{Tot}$	fmol	total soluble APPα
$sAPP\beta_{Tot}$	fmol	total soluble APPβ
K_A	$fmol^{-1}$	association constant of APP dimerization
K_B	$fmol^{-1}$	association constant of β-secretase dimerization
K_C	$fmol^{-1}$	association constant of α-secretase dimerization
K_s	$fmol^{-1}$	association constant of APP and SORLA
k_i	$fmol^{-1}\cdot h^{-1}$	binding rate constant (where i= 1, 3, 5, 31, 51)
k_j	h^{-1}	dissociation rate constant (where j= -1, -3, -5, -31, -51, -a, -b, -c, 4, 6, 41, 61)
k_h	$fmol^{-1}\cdot h^{-1}$	dimerization rate constant (where h= a, b, c)
$K_{M\alpha}$	fmol	defined by $(k_6+k_{-5})/k_5$
$K_{M\beta}$	fmol	defined by $(k_4+k_{-3})/k_3$
$K_{M\alpha_d}$	fmol	defined by $(k_{61}+k_{-51})/k_{51}$
$K_{M\beta_d}$	fmol	defined by $(k_{41}+k_{-31})/k_{31}$

A.2. Model equations

Ordinary differential equations (ODEs) describe temporal changes of molecular numbers for the network components as a function of interaction and cleavage processes. With large numbers of molecules, changes can be assumed to be smooth:

$$\left.\begin{aligned}
\dot{APP} &= -k_1 \cdot APP \cdot SORLA + k_{-1} \cdot C_{APPSORLA} - k_3 \cdot APP \cdot \beta + k_{-3} \cdot C_{APP\beta} \\
&\quad -k_5 \cdot APP \cdot \alpha + k_{-5} \cdot C_{APP\alpha} + 2 \cdot (k_{-a} \cdot APP_d - k_a \cdot APP^2) \\
\dot{SORLA} &= -k_1 \cdot APP \cdot SORLA + k_{-1} \cdot C_{APPSORLA} \\
\dot{\beta} &= -k_3 \cdot APP \cdot \beta + (k_{-3} + k_4) \cdot C_{APP\beta} + 2 \cdot (k_{-b} \cdot \beta_d - k_b \cdot \beta^2) \\
\dot{\alpha} &= -k_5 \cdot APP \cdot \alpha + (k_{-5} + k_6) \cdot C_{APP\alpha} + 2 \cdot (k_{-c} \cdot \alpha_d - k_c \cdot \alpha^2) \\
\dot{C_{APP\beta}} &= k_3 \cdot APP \cdot \beta - (k_{-3} + k_4) \cdot C_{APP\beta} \\
\dot{C_{APP\alpha}} &= k_5 \cdot APP \cdot \alpha - (k_{-5} + k_6) \cdot C_{APP\alpha} \\
\dot{sAPP\alpha} &= k_6 \cdot C_{APP\alpha} \\
\dot{sAPP\beta} &= k_4 \cdot C_{APP\beta} \\
\dot{C_{APPSORLA}} &= -\dot{SORLA} \\
\dot{APP_d} &= -k_{31} \cdot APP_d \cdot \beta_d + k_{-31} \cdot C_{APP_d\beta_d} - k_{51} \cdot APP_d \cdot \alpha_d \\
&\quad +k_{-51} \cdot C_{APP_d\alpha_d} - k_{-a} \cdot APP_d + k_a \cdot APP^2 \\
\dot{\beta_d} &= -k_{31} \cdot APP_d \cdot \beta_d + (k_{-31} + k_{41}) \cdot C_{APP_d\beta_d} + k_b \cdot \beta^2 - k_{-b} \cdot \beta_d \\
\dot{\alpha_d} &= -k_{51} \cdot APP_d \cdot \alpha_d + (k_{-51} + k_{61}) \cdot C_{APP_d\alpha_d} + k_c \cdot \alpha^2 - k_{-c} \cdot \alpha_d \\
\dot{C_{APP_d\beta_d}} &= k_{31} \cdot APP_d \cdot \beta_d - (k_{-31} + k_{41}) \cdot C_{APP_d\beta_d} \\
\dot{C_{APP_d\alpha_d}} &= k_{51} \cdot APP_d \cdot \alpha_d - (k_{-51} + k_{61}) \cdot C_{APP_d\alpha_d} \\
\dot{sAPP\alpha*} &= 2 \cdot k_{61} \cdot C_{APP_d\alpha_d} \\
\dot{sAPP\beta*} &= 2 \cdot k_{41} \cdot C_{APP_d\beta_d}
\end{aligned}\right\} \quad (1)$$

Note that the dot above variables denotes the time-dependent changes of the molecule numbers of these variables.

Since quasi-steady states can be assumed for the complexes, this allows the reduction of the equations. For example,

$$\begin{aligned}
\dot{C_{APP\alpha}} &= k_5 \cdot APP \cdot \alpha - (k_{-5} + k_6) \cdot C_{APP\alpha} \\
0 &= k_5 \cdot APP \cdot \alpha - (k_{-5} + k_6) \cdot C_{APP\alpha} \\
C_{APP\alpha} &= \frac{\alpha \cdot APP}{K_{M\alpha}}
\end{aligned}$$

Similarly for

$$C_{APP\beta} = \frac{\beta \cdot APP}{K_{M\beta}},\ C_{APP_d\alpha_d} = \frac{\alpha_d \cdot APP_d}{K_{M\alpha_d}}, C_{APP_d\beta_d} = \frac{\beta_d \cdot APP_d}{K_{M\beta_d}}$$

where $K_{M\alpha} = (k_6 + k_{-5})/k_5, K_{M\beta} = (k_4 + k_{-3})/k_3,\ K_{M\alpha_d} = (k_{61} + k_{-51})/k_{51},\ K_{M\beta_d} = (k_{41} + k_{-31})/k_{31}.$

We also take into account the association constants of APP, β-secretase, α-secretase dimerization and the rapid equilibrium assumption for the $C_{APPSORLA}$ complex that are denoted respectively as

$$K_A = \frac{APP_d}{APP^2}, K_B = \frac{\beta_d}{\beta^2}, K_C = \frac{\alpha_d}{\alpha^2} \text{ and } K_s = \frac{C_{APPSORLA}}{SORLA \cdot APP}$$

where $K_A = \frac{k_a}{k_{-a}},\ K_B = \frac{k_b}{k_{-b}},\ K_C = \frac{k_c}{k_{-c}},\ K_s = \frac{k_1}{k_{-1}}$. Note that the dissociation constant is the inverse of the association constant and vice versa (e.g. association constant K_A corresponds to dissociation constant K_A^{-1}).

Furthermore, the ODEs include conservation laws for the molecule numbers of enzymes and substrates. For α-secretase, β-secretase and SORLA this leads to

$$\alpha_{Tot} = \alpha + \frac{\alpha \cdot APP}{K_{M\alpha}} + 2 \cdot \left(K_C \cdot \alpha^2 + \frac{K_C \cdot \alpha^2 \cdot K_A \cdot APP^2}{K_{M\alpha_d}} \right)$$

$$\beta_{Tot} = \beta + \frac{\beta \cdot APP}{K_{M\beta}} + 2 \cdot \left(K_B \cdot \beta^2 + \frac{K_B \cdot \beta^2 \cdot K_A \cdot APP^2}{K_{M\beta_d}} \right)$$

$$SORLA_{Tot} = SORLA + \left(\frac{SORLA \cdot APP}{K_s^{-1}} \right) .$$

The first two equations can be transformed such that free molecule numbers of α-secretase (α) and β-secretase (β) can be calculated from α_{Tot} and β_{Tot} accordingly as:

$$\left.\begin{aligned}
\alpha &= -\frac{K_{M\alpha_d}\cdot(K_{M\alpha}+APP)}{4\cdot K_C\cdot K_{M\alpha}\cdot(K_{M\alpha_d}+K_A\cdot APP^2)} \\
&+\frac{\sqrt{K_{M\alpha_d}^2\cdot(K_{M\alpha}+APP)^2+8\cdot\alpha_{Tot}\cdot K_{M\alpha_d}\cdot K_C\cdot K_{M\alpha}^2\cdot(K_{M\alpha_d}+K_A\cdot APP^2)}}{4\cdot K_C\cdot K_{M\alpha}\cdot(K_{M\alpha_d}+K_A\cdot APP^2)} \\
\beta &= -\frac{K_{M\beta_d}\cdot(K_{M\beta}+APP)}{4\cdot K_B\cdot K_{M\beta}\cdot(K_{M\beta_d}+K_A\cdot APP^2)} \\
&+\frac{\sqrt{K_{M\beta_d}^2\cdot(K_{M\beta}+APP)^2+8\cdot\beta_{Tot}\cdot K_{M\beta_d}\cdot K_B\cdot K_{M\beta}^2\cdot(K_{M\beta_d}+K_A\cdot APP^2)}}{4\cdot K_B\cdot K_{M\beta}\cdot(K_{M\beta_d}+K_A\cdot APP^2)}
\end{aligned}\right\} \quad (2)$$

where only the positive solutions are biologically meaningful.

The ODEs that describe the formation of end products (as shown in Eqs.(1)) in the processing of monomeric and of dimeric forms of APP under the influence of SORLA can be rewritten in the following form (with the representation of α and β, in terms of α_{Tot} and β_{Tot} respectively, see Eqs. (2)):

$$\dot{sAPP\alpha} = k_6\cdot\frac{APP}{K_{M\alpha}}\cdot\alpha$$

$$\dot{sAPP\beta} = k_4\cdot\frac{APP}{K_{M\beta}}\cdot\beta$$

$$\dot{sAPP\alpha}^* = 2\cdot k_{61}\cdot\frac{K_A\cdot APP^2}{K_{M\alpha_d}}\cdot(K_C\cdot\alpha^2)$$

$$\dot{sAPP\beta}^* = 2\cdot k_{41}\cdot\frac{K_A\cdot APP^2}{K_{M\beta_d}}\cdot(K_B\cdot\beta^2)$$

From these equations we obtain

$$\dot{sAPP\alpha}_{Tot} = \dot{sAPP\alpha} + \dot{sAPP\alpha}^*$$

$$\dot{sAPP\beta}_{Tot} = \dot{sAPP\beta} + \dot{sAPP\beta}^* .$$

In addition, the ODEs include conservation of the APP substrate. This has also been confirmed experimentally (data not shown). The APP_{Tot} is a function of free APP ($APP_{Tot}(APP)$) and of APP bound in the complexes:

$$APP_{Tot}(APP) = APP\cdot\left(1+\frac{\alpha}{K_{M\alpha}}+\frac{\beta}{K_{M\beta}}+\frac{SORLA_{Tot}}{K_s^{-1}+APP}\right)+2\cdot(K_A\cdot APP^2)\cdot\left(1+\frac{K_C\cdot\alpha^2}{K_{M\alpha_d}}+\frac{K_B\cdot\beta^2}{K_{M\beta_d}}\right)$$

with the representation of α and β in Eqs (2).

A.3. Model parameter estimation

Parameter values were estimated by nonlinear optimization such that the model simulations fit four biological independent dose-response series without SORLA (a total of *N*=66 experimental data points) and five biological independent dose-response series with SORLA (also a total of *N*=66 experimental data points) by finding a set of parameter values that minimizes the weighted least squares function of $\dot{sAPP\alpha}_{Tot}$ and $\dot{sAPP\beta}_{Tot}$. Since the experimental values of sAPPα and sAPPβ are of different orders of magnitude, we assigned weights such that the influence of each data set in the process of optimization will be equal. The weights are defined as

$$w_a=\frac{\sum_{m=1}^{N}\dot{sAPP\alpha}_m^E}{N},\ w_b=\frac{\sum_{m=1}^{N}\dot{sAPP\beta}_m^E}{N},\ w_{aS}=\frac{\sum_{m=1}^{N}\dot{sAPP\alpha}_{S,m}^E}{N},\ w_{bS}=\frac{\sum_{m=1}^{N}\dot{sAPP\beta}_{S,m}^E}{N}$$

where the superscript '*E*' and the subscript '*S*' denotes experimental data points and the influence of SORLA, respectively. The goodness of fit was quantified by calculating the residual value, i.e. the sum of the squared differences between the data and model, divided by a respective weight:

$$residual=\min\sum_{k=1}^{N}\left(\frac{(\dot{sAPP\alpha}_k^E-\dot{sAPP\alpha}_{Tot,k})^2}{w_a}+\frac{(\dot{sAPP\beta}_k^E-\dot{sAPP\beta}_{Tot,k})^2}{w_b}+\frac{(\dot{sAPP\alpha}_{S,k}^E-\dot{sAPP\alpha}_{STot,k})^2}{w_{aS}}+\frac{(\dot{sAPP\beta}_{S,k}^E-\dot{sAPP\beta}_{STot,k})^2}{w_{bS}}\right)$$

We applied the `lsqnonlin` and `fzero` functions in the MATLAB optimization toolbox (*MATLAB*. Natick, Massachusetts: Math Works Inc.; 2009) to estimate unknown parameter values. Specifically, we used equations for $sA\dot{P}P\alpha$, $sA\dot{P}P\beta$ and $sA\dot{P}P\alpha^*$, $sA\dot{P}P\beta^*$ from monomer and dimer processing, and estimated the parameter values from dose response series. APP is calculated from the equation for APP_{Tot} using the `fzero()` function in MATLAB. The estimation has been performed by the following steps: (a) The initial values for the parameters are randomly assigned using the `rand()` function in MATLAB. (b) The initial values described in (a) are used for the `lsqnonlin()` function in MATLAB to estimate the parameter values of the mathematical equations. (c) Repeat (a) and (b) iteratively. (d) If the parameter values of the best fit are outside the boundaries of `rand()` then increase the boundaries and go back to (a).

A.4. Parameter values

Table A.4 Parameter values for Fig.11 B-E with residual = 2.15×10^{1}

parameter	**(units)**	**values**	**parameter**	**(units)**	**values**
α_{Tot}	(fmol)	7.34×10^{3}	β_{Tot}	(fmol)	6.05×10^{1}
$SORLA_{Tot}$	(fmol)	5.13×10^{5}	K_s	($fmol^{-1}$)	7.19×10^{-3}
K_B	($fmol^{-1}$)	2.10×10^{3}	K_C	($fmol^{-1}$)	7.41×10^{1}
K_A	($fmol^{-1}$)	1.25×10^{-1}			
Dimer processing			**Monomer processing**		
without SORLA					
k_{61}	(h^{-1})	4.75×10^{-1}	k_6	(h^{-1})	9.87×10^{-3}
$K_{M\alpha_d}$	(fmol)	5.51×10^{3}	$K_{M\alpha}$	(fmol)	4.32×10^{-2}
k_{41}	(h^{-1})	1.30×10^{-1}	k_4	(h^{-1})	1.16×10^{2}
$K_{M\beta_d}$	(fmol)	6.53×10^{1}	$K_{M\beta}$	(fmol)	2.93×10^{2}
with SORLA					
k_{61}	(h^{-1})	4.75×10^{-1}	k_6	(h^{-1})	9.87×10^{-3}
$K_{M\alpha_d}$	(fmol)	5.51×10^{3}	$K_{M\alpha}$	(fmol)	4.32×10^{-2}
k_{41}	(h^{-1})	1.30×10^{-1}	k_4	(h^{-1})	1.16×10^{2}
$K_{M\beta_d}$	(fmol)	2.19×10^{5}	$K_{M\beta}$	(fmol)	1.42×10^{1}

Note that only the parameters $K_{M\beta}$ and $K_{M\beta_d}$ were estimated locally and therefore differ in their values with and without SORLA.

In the combined model, where all parameters are estimated globally, about 75% of the fits show that alpha cleavage prefers dimer processing, while beta cleavage prefers monomer processing with and without SORLA. As shown experimentally (Fig. 8), SORLA does not interact directly with the α- and β-

secretases. It is for this reason that complex formation with the secretases is not considered in the model.

We performed 300 global estimates and 300 global-local estimates to compare the quality of both estimates. In the global-local fit, all parameters except $K_{M\beta}$ and $K_{M\beta_d}$ are estimated globally. Out of the 300 global-local estimation runs ($K_{M\beta}$ and $K_{M\beta_d}$ are estimated locally) and 300 global estimation runs, 214 and 216 fits are generated, respectively, satisfying the condition that all parameter values are positive. Note that none of the parameter values were taken from the literature due to the differences in the experimental methods applied. Thus, most kinetic data available in the literature on α/β-scereatse activity were obtained in cell free assays with purified enzyme and artificial peptide substrate. In contrast, our model relies in quantitative data obtained on APP processing in intact cells.

The model, where all parameters except $K_{M\beta}$ and $K_{M\beta_d}$ are estimated globally, supports the hypothesis of a switch from dimer processing in the absence of SORLA to monomer processing in the presence of SORLA in 80% of the global-local fits. This is in good agreement with our experimental finding that SORLA disrupts oligomerization of APP (Fig. 10). The other 20% of fits show beta cleavage prefers monomer processing in both, the absence and presence of SORLA.

The goodness of a fit was quantified by calculating the residual value, i.e. the sum of the squared differences between the data and model (see supporting information "*Model parameter estimation*"). Comparing global-local and purely global parameter estimates, the residual values for the best global fit (i.e. 30.26) are about 50% worse than the residual values of all the global-local estimation (as observed in Figure A.4). The residual values of all the 214 global-

local estimations are ranked from the lowest residual value of 21.5. A fit with a residual value smaller than 22 is considered a "good fit" Moreover, the global-local fits, where $K_{M\alpha}$ and $K_{M\alpha_d}$ are estimated locally, are a bit weaker (residual value 23.50) than the model presented in the manuscript, where $K_{M\beta}$ and $K_{M\beta_d}$ are locally estimated (residual value of 21.50), but better than the model where all parameters are fitted globally. This implies that the model, where all parameters except $K_{M\beta}$ and $K_{M\beta_d}$ are estimated globally, provides the best match to the experimental data. This observation also suggests a yet unidentified biological process whereby SORLA might indirectly affect the β-secretase, but not other secretases. This activity needs to be indentified in future experimental studies.

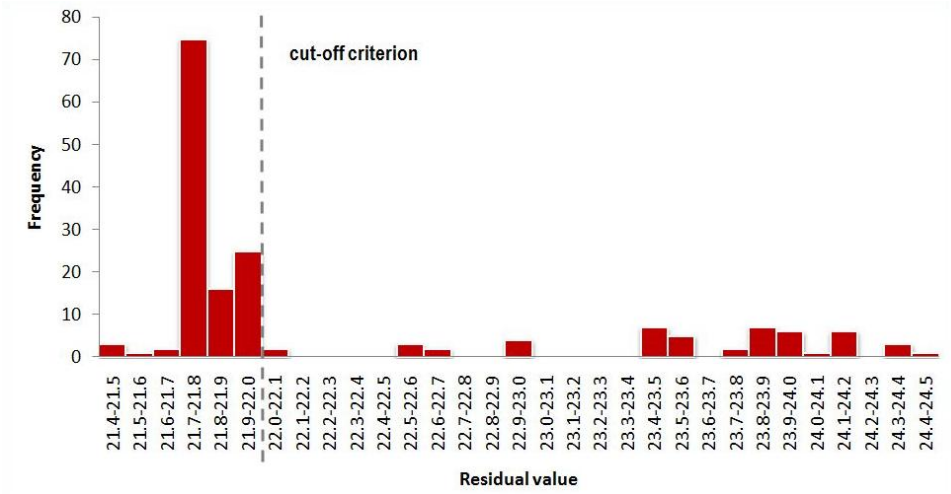

Figure A.4. Frequency distribution of the residual values of the 214 global –local fits. We have ranked the 214 global-local fits and have chosen 146 "good fits" starting from the lowest residuals. The distribution of residuals suggests an empirical cut-off criterion at 22. A fit with a residual value smaller than 22 is then considered a "good fit".

A.5. Intermediate levels of SORLA expression

We calculated the intermediate levels of SORLA expression between the cooperative and non-cooperative regimes in an indirect manner. Since the two parameters, $\boxed{K_{M\beta}}$ and $K_{M\beta_d}$ are fitted locally, the global-local estimation describes an indirect influence of SORLA.

Figure A.5 shows the empirically derived (almost exponential) dependencies of $K_{M\beta}$ and $K_{M\beta_d}$ on the intermediate levels of SORLA, where it is ensured that the simulations of the intermediate curves for $sAPP\dot{\alpha}_{Tot}$ and $sAPP\dot{\beta}_{Tot}$ (blue dashed curves Figure 12 A and B) stay smoothly in between the curves with and without SORLA (black curves in Figure 12 A and B). As we decreased the amount of SORLA, the intermediate curves stay smoothly in between with and without SORLA curves.

The simulations of the dose response curves of $sAPP\dot{\alpha}_{Tot}$, $sAPP\dot{\beta}_{Tot}$ (total processing in black curves), $sA\dot{P}P\alpha$, $sA\dot{P}P\beta$ (monomer processing in red curves) and $sA\dot{P}P\alpha^*$, $sA\dot{P}P\beta^*$ (dimer processing in green curves) for intermediate levels of SORLA expression are shown in Figure 12 (C-H). Interestingly, the switch between the cooperative and non-cooperative regimes occurs at low SORLA concentrations, i.e. ~0.12 x $SORLA_{Tot}$ (where $SORLA_{Tot}$ = 5.13 x 10^5 fmol, as shown in Table A.4).

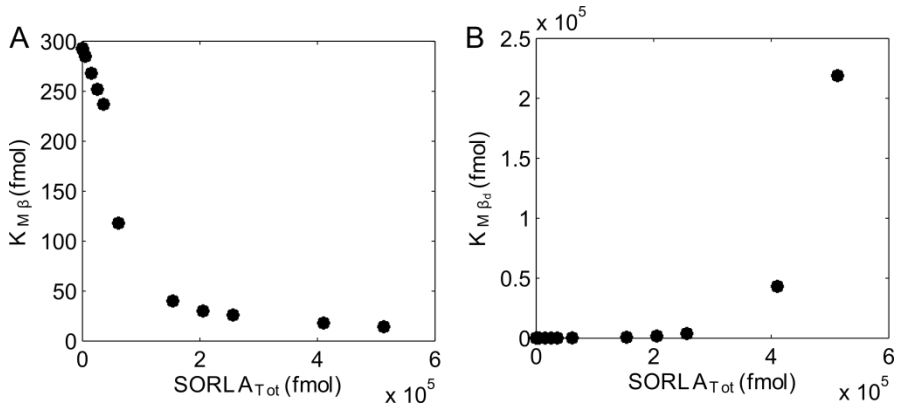

Figure A.5. Dependence of $K_{M\beta}$ and $K_{M\beta_d}$ on SORLA. The intermediate levels of SORLA expression are calculated in an indirect manner by empirically determining the dependencies of $K_{M\beta}$ (A) and $K_{M\beta_d}$ (B) on the intermediate levels of SORLA. These parameter values are used to simulate the dose-response kinetics of $\dot{sAPP\alpha}_{Tot}$, $\dot{sAPP\beta}_{Tot}$, $\dot{sAPP\alpha}$, $\dot{sAPP\beta}$ and $\dot{sAPP\alpha}*$, $\dot{sAPP\beta}*$ in dependence on intermediate levels of SORLA expression presented in Figure 12.

SUPPLEMENTARY FIGURES

Supplementary figure 1. Subcellular localization of APP and SORLA in CHO cells.

Localization of APP and SORLA was detected in the indicated cell lines treated or not treated with 1 ng/ml doxycycline for 48 hours. (**A**) Robust expression of APP in CHO pTet-APP (w/o Dox) is lost when cells are incubated with doxycycline (w/ Dox). (**B**) Strong colocalization of APP and SORLA is seen in the perinuclear region of untreated CHO-S pTet-APP cells (arrowheads; w/o Dox). Expression of APP (but not of SORLA) is lost upon treatment with doxycycline (w/ Dox). Scale bar: 20 μm.

Supplementary figure 2. Lack of endogenous expression of APP and SORLA in CHO cells.

Western blot analysis of APP and SORLA expression in lysates of parental CHO cells or CHO cells transfected with Tet-off constructs for APP (pTet-APP) or SORLA (pTet-SORLA). Cells were treated with 10 ng/ml of doxycycline for 48 hours prior to analysis. Detection of actin was used as loading control. Signals for APP and SORLA in the transfectants indicate residual expression of the transgene constructs. No immunoreactive bands corresponding to endogenous APP or SORLA are seen in the non-transfected parental cell line.

Supplementary figure 3. Detection of full-length and soluble APP variants in CHO cells.

Western blot analysis was used to detect APP variants in lysate and supernatant of CHO cells expression human APP_{695} (CHO- pTet-APP). A polyclonal anti-carboxyl

terminal APP antiserum (IgG1227) specific for full-length APP detects the precursor protein in the lysate but not in the medium of the cells. In the converse situation, IgG 2B3 specific for soluble (s) APPα detects the processing product in the medium but not in the cell lysate.

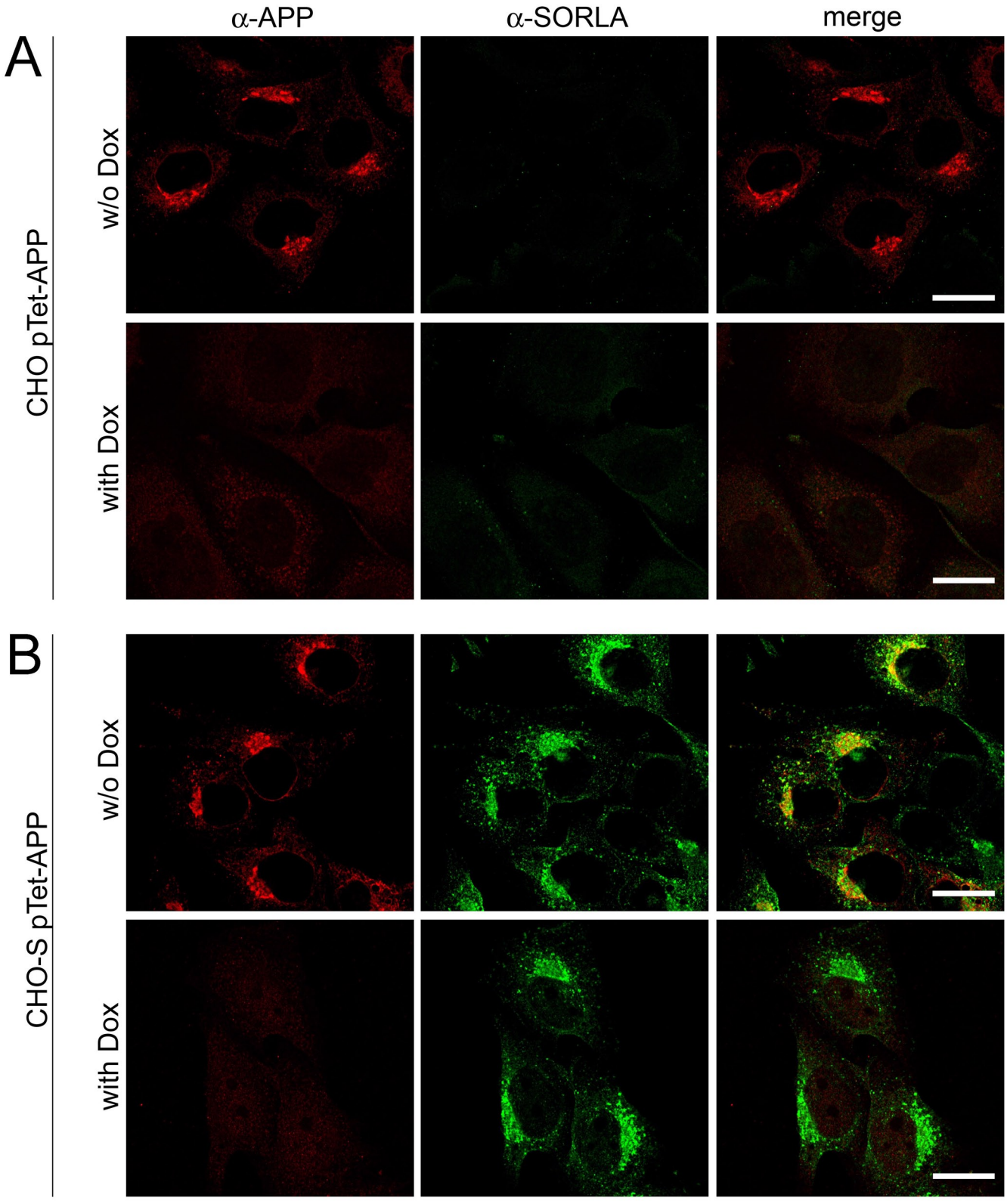

Schmidt et al.
Suppl. figure 1

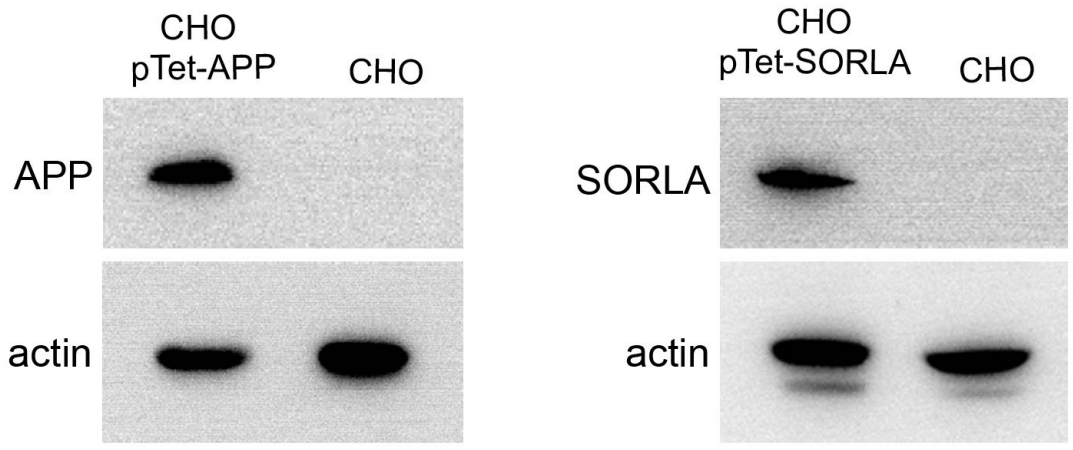

Schmidt et al.
Suppl. figure 2

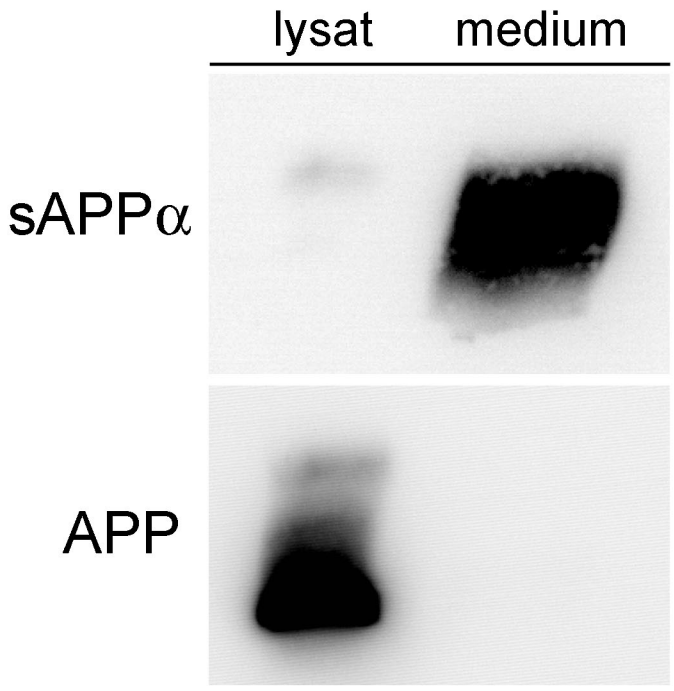

Schmidt et al.
Suppl. figure 3